DISSERTATIONES SCIENTIAE MATERIALIS UNIVERSITATIS TARTUENSIS

3

DISSERTATIONES SCIENTIAE MATERIALIS UNIVERSITATIS TARTUENSIS

3

MARGUS KODU

Pulsed Laser Deposition of Magnesium Oxide and Barium Ternary Oxides for Plasma Display Protective Layers

TARTU UNIVERSITY PRESS

Institute of Physics, Faculty of Science and Technology, University of Tartu, Estonia

Dissertation in Materials Science

The Dissertation was admitted on May 09, 2011, in partial fulfilment of the requirements for the degree of Doctor of Philosophy in materials science, and allowed for defence by the Scientific Council on Materials Science of the Faculty of Science and Technology of the University of Tartu.

Supervisors: Dr. Raivo Jaaniso, Institute of Physics,
University of Tartu

Opponents: Dr. Sanjay K. Ram, Department of Materials Science,
Faculty of Science and Technology,
Universidade Nova de Lisboa, Portugal

Dr. Sergei Bereznev, Department of Materials Science,
Faculty of Chemical and Materials Technology,
Tallinn University of Technology, Estonia

Commencement: July 7, 2011 at University of Tartu, Tartu, Estonia

Publication of thesis was supported by: Graduate School on Functional Materials and Technologies (GSFMT), University of Tartu and Tallinn University of Technology, EU Social Funds project 1.2.0401.09-0079

European Union
European Social Fund

Investing in your future

ISSN 2228–0928
ISBN 978–9949–19–689–0 (trükis)
ISBN 978–9949–19–690–6 (PDF)

Tartu Ülikooli Kirjastus
www.tyk.ee
Tellimus nr. 320

TABLE OF CONTENTS

LIST OF ABBREVIATIONS

ACC	alternating current coplanar
AC PDP	alternating current plasma display panel
AFM	atomic force microscopy
CL	cathodoluminescence
DBD	dielectric barrier discharge
EBD	electron beam deposition
EPMA	electron probe microanalysis
FV	firing voltage
ITO	indium tin oxide
LCD	liquid crystal display
OLED	organic light emitting diode
PDP	plasma display panel
PLD	pulsed laser deposition
PL	photoluminescence
SEE	secondary electron emission
TL	thermoluminescence
UV	ultraviolet
VUV	vacuum ultraviolet
XPS	x-ray photoelectron spectroscopy
XRD	x-ray diffraction
XRR	x-ray reflection

LIST OF PUBLICATIONS

Publications on which the thesis is based

I. V. Denks, M. Aints, T. Avarmaa, J.S. Choi, E. Feldbach, R. Jaaniso, A. Kasikov, M. Kirm, M. Kodu, M.S. Lee, A. Maaroos, Y.T. Matulevich, H. Mändar, J. Raud, *Investigation of Possible Replacement of Protective Magnesium Oxide Layer in Plasma Display Panels by Barium Ternary Oxides*, J. Phys. D: Appl. Phys. 40 (2007) 4503–4507.

II. M. Kodu, T. Avarmaa, H. Mändar, R. Jaaniso, *Pulsed Laser Deposition of* $BaGa_2O_4$, Appl. Phys. A 93 (2008) 801–805.

III. E. Feldbach, R. Jaaniso, M. Kodu, V. P. Denks, A. Kasikov, P. Liblik, A. Maaroos, H. Mändar and M. Kirm, *Luminescence Characterization of Ultrathin MgO Films of High Crystallinity Prepared by Pulsed Laser Deposition*, Journal of Materials Science: Materials in Electronics 20 (2009) 321–25.

IV. M. Kodu, J. Raud, M. Aints, T. Avarmaa, V. Denks, J.S. Choi, E. Feldbach, R. Jaaniso, M. Kirm, M.S. Lee, A. Maaroos, Y.T. Matulevich, H. Mändar, V. Sammelselg, *Structural and Discharging Properties of MgO Thin Films Prepared by Pulsed Laser Deposition*, Thin Solid Films 519 (2010) 846–851.

V. M. Kodu, J. Raud, M. Aints, T. Avarmaa, V. Denks, E. Feldbach, R. Jaaniso, M. Kirm, A. Maaroos, *Hydrogen doping of MgO thin films prepared by pulsed laser deposition*, Applied Surface Science 257 (2011) 5328–5331.

Publications not directly connected to the subject of this thesis

VI. I. Kärkkänen, M. Kodu, T. Avarmaa, J. Kozlova, L. Matisen, H. Mändar, A. Saar, V. Sammelselg, R. Jaaniso, *Sensitivity of CoWO4 thin films to CO*, Procedia Engineering 5 (2010) 160–163.

VII. K. Kruusamäe, P. Brunetto, S. Graziani, L. Fortuna, M. Kodu, R. Jaaniso, A. Punning, A. Aabloo, *Experiments with self-sensing IPMC actuating device*, Proceedings of SPIE (2010) (76420V).

Author's contribution

In all the listed papers, the author was responsible for selecting the deposition conditions and depositing all the thin film samples. All firing voltage measurements were made by Dr Jüri Raud. The author's contributions to the rest of activities (planning of experiments, sample analysis, writing of paper) for each paper are as follows:

Paper I:	The author made AFM measurements, participated in the data analysis.
Paper II:	The author was responsible for the planning of the experiments. Actively participated in the data analysis and in the preparation of the manuscript.
Paper III:	The author participated in the data analysis.
Paper IV:	The author was responsible for the planning of the experiments, made all the XRD, XRR and AFM measurements, was responsible for the data analysis and the preparation of the manuscript.
Paper V:	The author actively participated in the data analysis, was responsible for the preparation of the manuscript.

1. INTRODUCTION

Today, large-screen displays are constantly being developed by electronics manufacturers to make them larger, more efficient and to enhance the picture quality of the screen. Until now, there were two main competitive flat display screen technologies – liquid crystal display (LCD) and plasma display panel (PDP), however, recently a new promising screen technology has emerged – organic light-emitting diode (OLED) display technology. Some of the display manufacturers have concentrated their production and development on plasma displays only.

Compared to LCDs, the competitors of PDPs, PDPs offer advantages in the picture quality: higher contrast ratio, wider viewing angles, more perfect performance when displaying the content with large amounts of rapid motion. In addition, PDPs have advantages in a very large screen display (> 100 inch) market and hold the record of the world's largest television set of 152 inches.

Some of the disadvantages of PDPs were, and partly still are, their relatively large power consumption and low cost effectiveness. Besides other elements that most of all influence the PDP characteristics, the thin layer of MgO in plasma screen is one of the key elements in PDPs and its properties have great influence on the display's image quality, its lifetime, cost and power consumption.

To improve the properties of this MgO layer or to find a replacement material with better properties, a cooperation project between the consumer-electronics manufacturer Samsung SDI and Institute of Physics was launched. The topic of this thesis originates from the project between Samsung SDI and Institute of Physics and partly contains the work carried through and the results obtained under the project.

In this work, the morphological and defect structure of MgO thin films was modified by varying film synthesizing conditions. The influence of these modifications on films' characteristics was studied from the standpoint of PDP applications. Some possible replacement materials for MgO were also investigated. The main attention was turned to the materials group of barium ternary oxides. The thin films, investigated in this work, were all synthesized by the pulsed laser deposition (PLD) method.

A short overview of the history and the construction of the plasma display and also an introduction of the PLD method is given in Chapter 2. In Chapter 3, the main objectives of this thesis work are outlined. A closer look at the experimental techniques used in this work is made in Chapter 4. Chapter 5 covers the work done on the modifying the morphological and defect structure of MgO and Chapter 6 describes the investigation of some possible MgO replacement materials.

2. BACKGROUND AND CONCEPT

2.1. Plasma display panels

A plasma display panel is a matrix of sub-millimeter discharge cells that are controlled by electronic drivers [1]. The displayed image is made up of millions of pixels each of which consists of three elementary discharge cells. The ultraviolet (UV) light emitted by the discharge cells is converted into a visible light of primary colors by phosphors in each cell. An alternating current plasma display panel (AC PDP) uses dielectric barrier discharges (DBD) to create plasma in each cell. The discharges operate in a glow regime in a rear gas mixture. The typical cell parameters are 500 Torr pressure and 100 μm gap length. Typically, a rectangular AC voltage with the frequency of the order of 100 kHz is used.

Two scientists, Bitzer and Slottow, working in the Coordinated Science Laboratory in the University of Illinois, invented the PDP in the 1960s. PDPs were first developed for displaying computer-generated images for educational purposes.

Initially, the PDPs were monochrome devices in which light source was gas-discharge created in a Ne-Ar (0.1% Ar) gas mixture. The light was a red-orange emission of Ne. These displays were used by professionals and military for displaying complex images.

In 1970s, the development of color PDPs was started and the first commercial color display was introduced in the late 1990s. The UV light emitting Xe-Ne or Xe-Ne-He gas mixture is used in color PDPs. The UV light is absorbed by three kinds of phosphors that emit three basic colors. A number of PDP designs have been proposed during 30 years. The most successful, and the one that is being used today, has been the alternating current coplanar (ACC) structure (Figure 1). In the ACC design, sustain discharges occur between the two parallel electrodes placed on the same plate. Addressing is provided by an electrode placed at the opposite plate and the address electrode is orthogonal to sustain electrodes. Every cell contains microscopic DBD, i.e. electrodes are coated with 20–40 μm thick dielectric layer (lead-rich glass). The plasma display consists of two glass plates separated by an about 100 μm gap filled with a rare gas mixture. Electrode arrays are deposited on both glass plates. Coplanar electrodes (also called display electrodes) are made of a transparent conductive oxide material (indium tin oxide – ITO). Since the resistivity of ITO is not zero, then every ITO electrode is attached to a narrow metal electrode called bus electrode. Data (or address) electrodes are metallic. The successive pairs of coplanar electrodes are separated by a dielectric barrier strip. The gap between the electrodes is about 100 μm and gas pressure is about 500 Torr. At these conditions, the pd (pressure × gap length) value of the cell is a couple of Torr × cm and the discharge remains in the glow discharge regime. It is important to work in that regime because it allows the controlling of discharge parameters and to achieve the process repeatability.

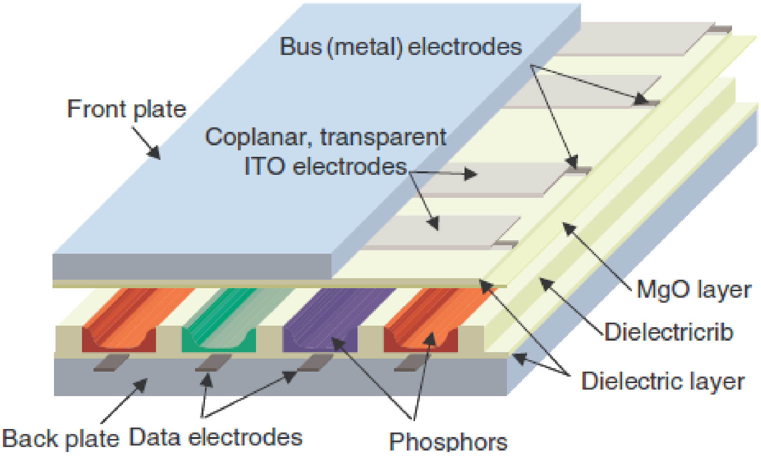

Figure 1. Simplified view of a coplanar PDP (after Boeuf [1]). The observer is on the front plate side.

An about 500 nm thick MgO film is deposited on the dielectric layer that covers coplanar electrodes. The MgO film protects the dielectric layer from plasma erosion and at the same time ensures a large secondary-electron emission (SEE) under the ion impact. The main issues of the PDP industry have been the efficiency, the lifetime, the manufacturing cost and, naturally, the image quality. Each of these subjects is related to the properties of the MgO film on the dielectric layer and because of this the MgO layer is the key element of PDPs.

The gas mixture commonly used in color PDP is the Xe-Ne mixture (3–10% Xe). Xe is used as a vacuum ultraviolet (VUV) emitter and the buffer gas Ne is used for lowering the breakdown voltage (because of the large Ne-ion-induced secondary electron emission (SEE) coefficient of MgO).

2.2. Properties of MgO and its role in plasma displays

Magnesium oxide occurs naturally as the mineral periclase and is prepared commercially by thermally decomposing the mineral magnesite: $MgCO_3$ (s) → MgO (s) + CO_2 (g). MgO is an ionic crystal that has face centered cubic structure (space group Fm3m) with lattice parameter 0.4212 nm. Some of its properties are: density – 3.58 g/cm^3, melting point – 2826 ^{o}C, refractive index – 1.74 (at 589 nm), band gap – 7.8 eV.

The MgO film is the key element in plasma displays. It protects the dielectric layer on the electrodes from ion sputtering and at the same time it ensures a large ion- induced secondary-electron emission coefficient for Ne^+ ions. Due to the large SEE coefficient and high sputtering resistance, MgO is essential for keeping the operating voltage low and to ensure a low wear under ion bombardment. Therefore, MgO has a substantial role from the aspects of efficiency (power consumption) and lifetime. MgO is a unique material due to its appropriate combination of emissive and protective properties. This explains the fact that this material was used already in 1970s [2] and is also used today in PDP industry, despite of many attempts to find a material with better properties.

2.3. Measurement of the SEE yield

The ion-induced SEE coefficient γ can be defined as the number of electrons that are emitted from the cathode per incident ion. Two techniques are used to measure the materials' SEE coefficient: ion beam measurements and estimation of γ from breakdown voltage (or firing voltage – FV) measurements [1]. The ion beam based methods are difficult to perform and require a sophisticated apparatus. In the current work, the breakdown voltage measurement method is used. In that case, only the effective SEE coefficient can be obtained, which includes the effects of ions, metastable species and photons. The yield of secondary electrons determines the firing voltage of glow discharges in a DBD cell [3]:

$$FV = 2.72\frac{g}{h}\ln(1+\frac{1}{\gamma}), \qquad (1)$$

where g and h are the constants dependent on the discharge gas composition, γ is the yield of the secondary electron emission. The firing voltage decreases as the yield of the secondary electron emission increases. The value of SEE coefficient also influences directly the sustain voltage of the DBD cell. The energy dissipated in a discharges of the plasma display is proportional to the square of sustain voltage of the cells (power consumption ~ (sustain voltage)^2).

For achieving our goals in this work, it is not necessary to evaluate the precise values of the SEE coefficient γ, while a comparison of the breakdown voltage values of the samples will suffice. For that reason the SEE coefficients of the samples were not calculated, but FV values were taken as a basis to estimate the suitability of different materials.

2.4. Theoretical background of the SEE coefficient

The theory of the electron emission due to Auger ejection of electrons states that the secondary emission by low-energy ions depends mainly on the potential energy of ions and is not influenced by their kinetic energy. For insulating surfaces, the secondary emission yield due to Auger emission is a combination of (a) Auger neutralization, and (b) a resonance neutralization process followed by Auger de-excitation [1, 4]. Auger neutralization secondary electron emission yield does not depend on the surface work function, but on the sum of the band gap E_g and the electron affinity χ of the insulator surface, and on the ion internal energy E_i. The emission of electrons by the Auger neutralization process is non-zero when the parameter

$$G = E_i - 2(E_g + \chi) \quad (2)$$

is positive and increases with the increasing of G. If Eg = 7.8 eV and $\chi = 0.85$ eV (as for MgO), then G is positive for Ne^+ ($E_i = 21.6$ eV) ions (process 1+3 in Figure 2) and negative for Xe^+ ($E_i = 12.1$ eV) ions (process 2+3 in Figure 2) on MgO. A theoretical γ due to the ion impact is determined to be 0.29 for Ne^+ and 0 for Xe^+ ions [1]. This is a very important result, since Xe^+ ions are the dominant species in the PDP discharge.

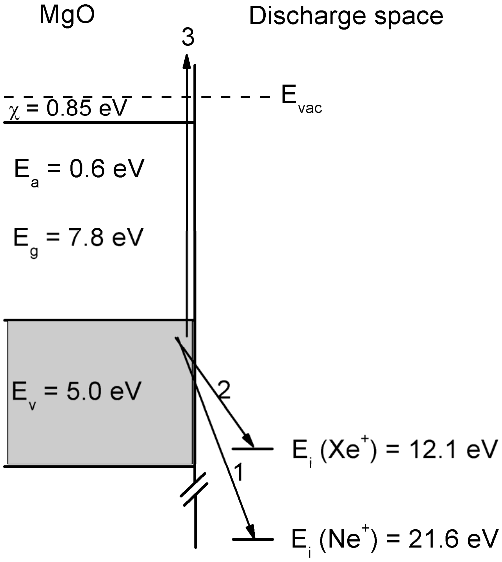

Figure 2. Simplified energy level diagram showing the involved MgO, Ne, and Xe energy levels relative to the vacuum level and the possible Auger emission processes.

2.5. The pulsed laser deposition method

Pulsed laser deposition (PLD) is a thin film deposition method in which the bulk starting material is vaporized (or ablated) by using the photonic energy of the laser beam [5, 6]. The principle of PLD is depicted in Figure 3. An intense pulse of the laser light is guided to the deposition chamber through an optical window and focused on a liquid or solid surface (the target) in which the beam is partly absorbed. Above a certain power density, the material of the target surface volatilizes in the form of luminous plume. The threshold power density of plume formation depends on the target material, its morphology, laser wavelength and laser pulse duration. For an UV excimer laser with ~10 ns pulse, the threshold power density lies between 10 and 500 MW/cm^2. The constituent material of the plume is allowed to condensate on an appropriate substrate, on which the growth of the film occurs. The film deposition process is often carried out in an atmosphere of a chemically active or passive background gas that influences the processes in the expanding plasma plume or on the growth substrate.

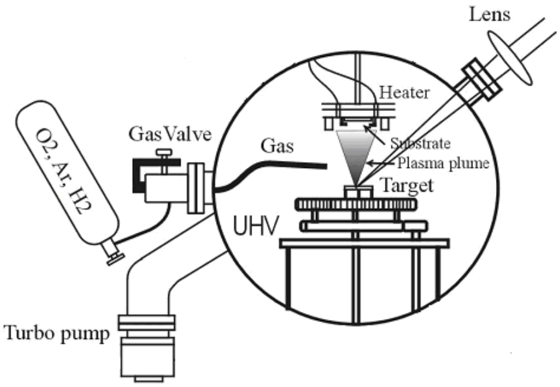

Figure 3. Principle schematic of a typical pulsed laser deposition setup. (This figure is reprinted by the permission of Taavi Jantson)

When the laser pulse is absorbed by the target surface, the electromagnetic energy is converted immediately into electronic excitations in the form of plasmons, unbound electrons and excitons. The excited electrons transfer their energy to the crystal lattice within a few picoseconds and the heating of the material begins within the optical absorption depth. In the ablation of a multi-elemental target, a congruent evaporation is possible only if the thermal diffusion length is smaller than the optical absorption length and then it is possible to obtain films with an elemental composition identical to the target's composition.

One of the biggest advantages of the PLD method is the possibility of finding the deposition conditions at which the elemental composition of the plasma plume exactly matches the composition of the target (congruent evaporation). This can be explained by the highly thermally nonequilibric nature of the process. The laser pulse with a nanosecond duration causes a fast heating of the target surface because of the high absorption coefficient or low thermal conductivity of the target. Therefore, the material is evaporated before it segregates to different phases that can have very different vapor pressures. This the so-called transfer of stoichometry between the target and the substrate allows the using of this method for depositing films with complex composition, such as superconductors, ferroelectric perovskites and transparent conductive oxides.

Immediately after the laser pulse, plasma is confined in a small volume and it can have temperatures in excess of 20 000 K. The degree of the ionization of the freshly-formed plasma can be in the range of 0.1–1. It consists of atomic, molecular and ionic species and of free electrons. The temperature and the degree of the ionization of the plasma are reducing during its adiabatic expansion.

The expansion of nascent plasma is strongly influenced by the background gas, which is often used during the deposition to modify the film growth processes. For instance, the collisions with the background gas influence the kinetic energy and quantity of the plasma species arriving to the growth substrate and also the shape of the expanding plume. Chemical reactions between gas and plasma species may modify the composition of the depositing material. Oxides are often grown in the oxygen gas to compensate for the loss of the oxygen component caused by a somewhat incongruent ablation.

In PLD, the ablation plasma is characterized by a high degree of ionization and high kinetic energies of the species. Kinetic energies may be between 1–500 eV (typically 5–50 eV), depending on laser pulse parameters. When arriving on the substrate, these species with high kinetic energies can have positive or negative influence on the quality of the growing film. They may improve or worsen the morphology, stoichometry and microstructure of the film. Usually, appropriate growth conditions are selected to keep kinetic energies low enough to prevent the breaking of atomic bonds and the production of vacancies and other crystallographic defects. However, relatively high kinetic energies of the plasma particles may improve the quality of the film because of the enhanced surface mobility and reactivity.

When a deposition process is carried out in a gas atmosphere, then, in addition to collisions among themselves, species in the plasma plume collide with background gas molecules. These collisions reduce the degree of the ionization and the kinetic energy of the ablation plasma. At high gas pressures, impinging plasma species lose most of their kinetic energy and plasma thermalizes before the species arrive at the substrate and their mobility on the substrate is insufficient for obtaining a high-quality crystal structure. In that case, the heating of the growth substrate for enhancing the mobility of the atomic species is necessary for obtaining films with a high-quality crystal structure.

The quality and other properties of the films grown with PLD are dependent on a number of growth parameters. The most important ones with their typical values used are as follows:

- laser wavelength (usually UV: 193 or 248 nm)
- laser energy density at the target (1–10 J/cm^2)
- laser pulse length
- laser pulse frequency (1–10 Hz)
- background gas (O_2, Ar, N_2, H_2)
- background gas pressure (10^{-4} – 100 Pa)
- density and morphology of the target (monocrystal, ceramics)

- distance between target and substrate (2–10 cm)
- substrate temperature (20–1000^{o}C)

The PLD method has a number of advantages:

- the energy source is positioned outside the vacuum chamber, which offers flexibility when considering the materials selection and the system geometry
- a possibility to deposit almost any material which is in a condensed state
- an accurate control of film thickness and growth rate
- the location of material vaporization is precisely defined by the laser focus spot
- in the regime of optimum deposition conditions, the chemical composition of the target and the film are identical even in the case of chemically complex materials
- the ability to produce species with electronic states far from the chemical equilibrium opens up the potential to produce novel or metastable materials that would be unattainable under thermal conditions

The PLD method has also some drawbacks that have to be considered when choosing deposition conditions:

- the production of macroscopic particles during the ablation process
- plasma species with high kinetic energy may generate crystallographic defects in a growing film
- inhomogeneous flux and angular energy distributions within the ablation plume

To conclude, the PLD method is quite unique from the aspect of the possibility to deposit films of a large variety of materials and to greatly modify the structure and, hence, the properties of the growing film by varying the deposition conditions. It is also important to note that PLD allows the doping of films, which is made easily by introducing a suitable dopant at definite concentrations to the target material. These considerations allow a conclusion that the PLD method is a good choice for a systematic study of the materials improvement.

3. GOALS OF THE RESEARCH

The main objective of this study was to discover potential ways for improving the discharging properties of the plasma display protective layer. There are two ways for improving the properties of a certain functional coating: by replacing the earlier used material by new material with better properties regarding the given application, or by modifying the currently-used material to further improve its useful properties. In this thesis work, both approaches have been attempted: first, the influence of modifying the morphological and energy level structure of MgO thin films on discharge properties has been studied, and second, some possible replacement materials to MgO protective coating have been chosen and examined.

The morphological and defect structure of MgO thin films are both important factors that influence the firing voltage value of the discharge cells in plasma display panel. Therefore, gaining more information about the relation of these properties is essential for the improvement of the discharging properties of plasma display cells and for lowering of its power consumption. Also, the possibility of replacing the MgO protective layer with an alternative material should be considered. If promising samples of these materials are found, then the properties of these materials could be engineered to outmatch those of the MgO's.

Further particular objectives of the study were:

- The investigation of the intrinsic defects of laser-deposited MgO thin films. For that purpose a series of MgO films was synthesized and their luminescence properties were studied by cathodoluminescence and photoluminescence spectroscopy methods.
- The establishment of relations between the growth conditions, structural properties and discharging characteristics of the MgO protective layer. To achieve that goal, a series of undoped MgO thin films were deposited and their structural and discharging properties were studied.
- The doping of MgO with impurities in order to further improve the MgO coating properties. Because of the hydrogen impurity's ability to introduce electron traps into a MgO crystal, it was considered as a promising candidate. Also, considering that this dopant has not been well investigated from the point of view of thin films and their discharge properties.
- Choosing some previously unexplored but potentially promising materials and investigating their possible suitability for a PDP protective layer candidate. For that purpose, two barium ternary oxides were chosen, their films were synthesized and their properties were investigated.

4. EXPERIMENTAL TECHNIQUES

4.1. Pulsed laser deposition of thin films

In this work, thin films were deposited by the PLD method on four types of substrates: (a) 10x10 mm Si (1 0 0) substrates for structural characterization and thermoluminescence measurements, (b) 22x35 mm special substrates for FV measurements (Figure 4), (c) 10x10 mm fused silica and (d) Pt(111)/Ti/SiO_2/Si substrates for a structural characterization. Prior to the deposition the substrates were cleaned as follows: Si(1 0 0) substrates – (a) the organic impurities were removed in a piranha process (H_2O:H_2SO_4:H_2O_2 solution); (b) the substrates were HF etched to remove the SiO_2 layer, leaving H-terminated Si surface, SiO_2 substrates – (a) the organic impurities were removed in a piranha process (H_2O:H_2SO_4:H_2O_2 solution); (b) the substrates were processed in ultrasonic bath in acetone; (c) finally, the substrates were rinsed by methanol, electrode substrates and Pt(111)/Ti/SiO_2/Si substrates – (a) rinsing in acetone followed by (b) rinsing in methanol.

Before starting the deposition, the chamber was always evacuated to a base pressure $<2\times10^{-4}$ Pa and the substrate temperature was raised to the chosen value. Oxygen was always introduced into the chamber after the base pressure and the substrate temperature were reached. The thickness of the growing film was monitored during the deposition process by optical reflectance. The Si and SiO_2 substrates with deposited films were stored in a dry air atmosphere for further analysis. The samples for FV measurements were inserted into the FV measurement chamber immediately after their removal from the PLD chamber in order to minimize the exposure to ambient atmosphere.

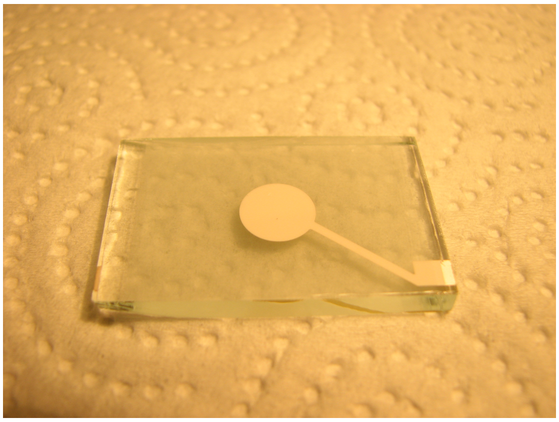

Figure 4. Electrode substrate for firing voltage measurements.

The laser deposition system used for synthesizing thin films is represented in Figure 5. The cylindrically-shaped vacuum chamber is made of stainless steel and is equipped with several connection flanges. A rotary vane pump Alcatel PASCAL 2015 C1 is used as the pre-vacuum pump and a turbomolecular pump Pfeiffer TMU 260 is used as the high-vacuum pump to reach the desired vacuum level in the chamber. A peumatically actuated gate valve is positioned between the turbopump and the chamber. A full-range vacuum gauge Balzers PKR 260 ($5*10^{-6}$–100000 Pa) is used to measure the pressure in the chamber. It consists of a Pirani-type gauge and a cold-cathode gauge. The additive gas is leaked to the chamber through a gas-dosing valve Balzers UDV 140. The reading of Balzers full range gauge is used as a feedback parameter to control the gas pressure during the deposition process, but the exact value of the additive gas pressure is measured by a capacitive-type MKS Baratron vacuum meter.

A Coherent Compex Pro 205 KrF excimer laser (wavelength 248 nm, pulse width 25 ns) is used for ablation. The maximum laser pulse energy is 750 mJ. The laser is capable of working in the 1–50 Hz pulse frequency range. The laser beam is guided to the deposition chamber by several dielectric mirrors and is focused on the target surface by fused silica lens. The energy of the laser pulse may be regulated from the laser control panel (through laser discharge voltage value) and by using a variable attenuator in the path of the laser light.

An Aja International SHQ400 series heater is used to raise the temperature of the growth substrate. The heater block, made of a 6 mm thickness and 60 mm diameter heat- resistant Inconel alloy metal slab, is heated by two quartz lamps which are surrounded by a water-cooled reflector. The temperature of the heater block is measured by using a thermocouple and controlled by a proportional–integral–derivative (PID) controller. The heater allows the reaching of the temperatures up to 950 ^{o}C at a normal oxygen pressure.

The substrates are fixed on a heater block by using a mask, which is made of 0.6 mm Inconel sheet metal. The mask has a hole with appropriate dimensions in a suitable location, that allows fixing the substrate in place. The mask is needed for two reasons: it holds the substrate in place by pressing it against the heater block and at the same time it works as a heat-reflecting screen.

A mechanical carousel-type manipulator, that can hold up to 3 targets, realizes the target selecting and scanning during the growth process. The carousel is moved by step- and servomotor. The PLD process is operated by a control computer, which runs a deposition system’s control software.

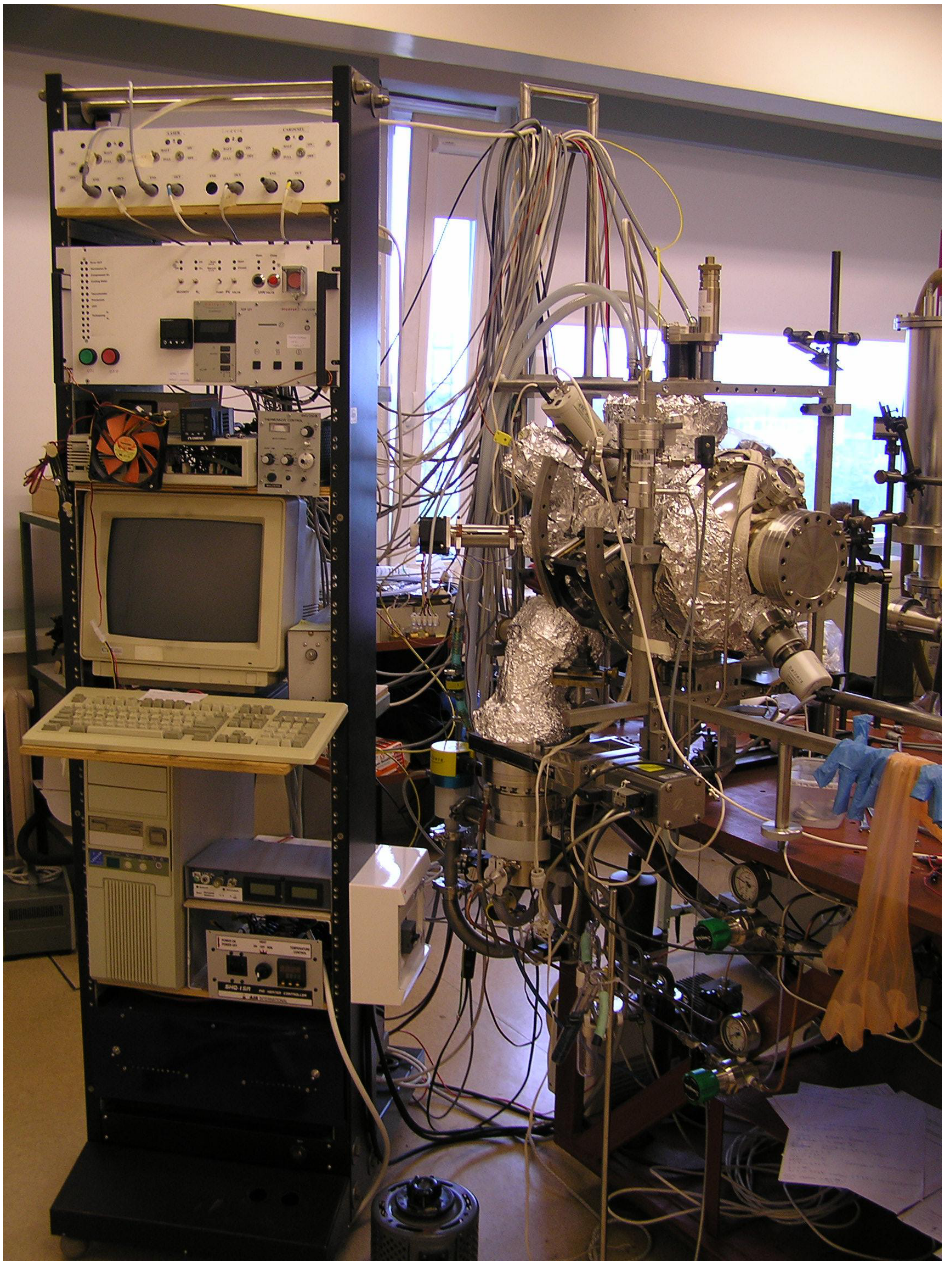

Figure 5. PLD system used in this work.

4.2 Film characterization methods

The structural and the morphological characterization of the films was performed by *ex-situ* x-ray diffraction (XRD), x-ray reflection (XRR), and atomic force microscopy (AFM) methods. The tapping mode AFM measurements were made by using a Veeco CP-II scanning probe microscope. The XRD analysis was performed on a Bragg–Brentano diffractometer DRON-1 (Nauchpribor) in a symmetrical coupled $\theta/2\theta$ step-scanning mode. An x-ray beam from a fine focus x-ray tube (Cu Kα radiation), working at 40 kV and 20 mA, was detected with a NaI:Tl scintillation detector. XRR was performed on a reconstructed topographic diffractometer URT–1 (Nauchpribor) by using Cu Kα radiation from a fine-focus x-ray tube. The slit collimation of the x-ray beam resulted in a value of 0.036° (in 2θ) for the full width at half maximum of the primary beam. Reflection patterns were collected in a step-scanning mode from 0.15° to 4° in 2θ. The X-ray data analysis was performed with the AXES software [7]. The thickness, roughness and density of the films were determined from the XRR data on the basis of the Parratt's recursive relation [8].

Low-temperature thermoluminescence (TL) measurements were performed by using a tunable electron beam excitation in the range of 1–30 keV, which allows the adjustment of the penetration depth of the exciting electrons in accordance with the film thickness. The integrated luminescence in the range from 185nm to 650nm was detected by using a Hamamatsu H5783-03 photomultiplier after the electron beam (0.1 μA, 5 keV) irradiation during 10 min. The heating rate of 10 K/min from 5K to 400K was used in thermoluminescence measurements. For low-temperature cathodoluminescence (CL), the light was analyzed by two double monochromators, which cover the range from 4.5–11.5 eV (vacuum grating monochromator) and 1.7–6 eV (UV-visible prism instrument), respectively.

4.3 Firing voltage measurements

A sample for the FV measurement consisted of a glass substrate (see Figure 6, where the cross-section of a sample is depicted), an Ag metal electrode screen-printed on the glass substrate, a dielectric layer above the electrode, and an MgO layer on top of the dielectric. The dimensions of the glass substrate were 22x35x3 mm, the diameter of the evaporated electrode was 8 mm, and the thickness of the dielectric layer made from a lead-rich glass was about 25 μm. The discharge cell was formed of two samples with identical MgO films (deposited in the same process) placed against each other with a gas gap of 0.12 mm between them.

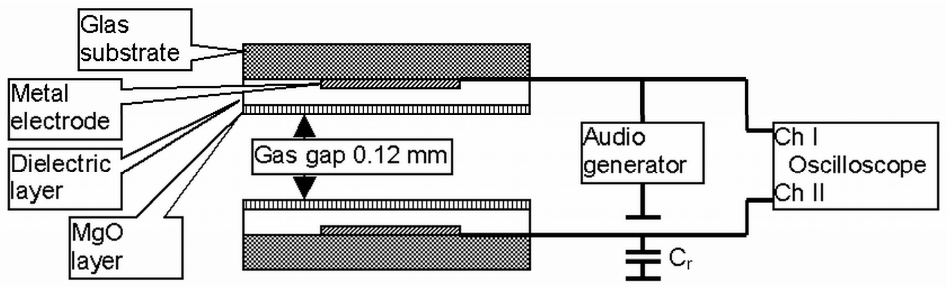

Figure 6. Discharge cell and electric circuitry for FV measurements.

The discharge cell was mounted into an ultra-high-vacuum-compatible stainless steel chamber with a window for visual observation. The chamber was evacuated down to a base pressure of ~10^{-6} Pa and then filled with a purging gas (argon 99.999%) three times before the initial aging procedure. A gas mixture of Ne and 10% Xe (purity of both gases 99.999%) at the pressure of 46 kPa was used for aging as well as for FV measurements. For aging, the AC voltage with a frequency of 30 kHz and with an amplitude surpassing that of the ignition voltage by about 10 V, was applied to the discharge cell during an hour. The gas was changed again after the aging procedure was completed and the FV measurements were started. The FV measurements were carried out with the AC frequency that was changed between 2 and 30 kHz. The discharge firing was detected and the Lissajous figures (Figure 7) were recorded with a digital oscilloscope (Tektronix TDS 3032) connected as shown in Figure 6.

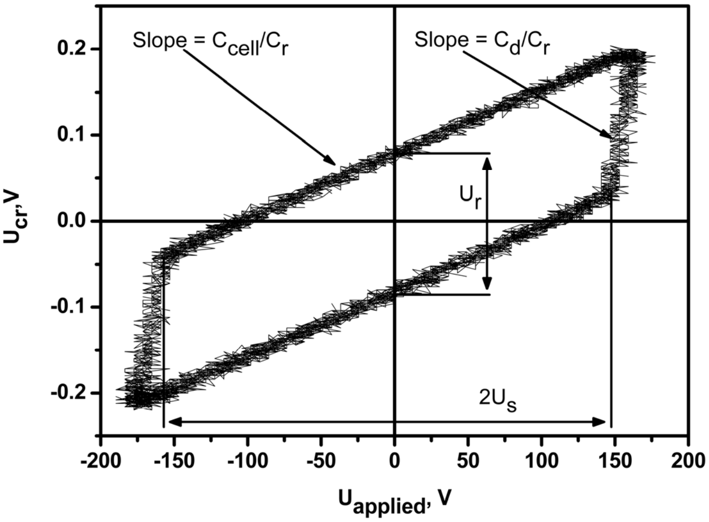

Figure 7. A typical Lissajous figure.

The firing of the plasma results in the charge transfer between the cell and the reference capacitor C_r. The plotting of the voltage U_r measured across C_r (voltage recorded by channel II of the oscilloscope in Figure 6) against the total voltage U_a applied to the system (recorded by channel I of the oscilloscope in Figure 6), results in a straight line without a discharge and in a 'Lissajous'-like figure (Figure 7) as soon as the discharge is ignited. On increasing the applied voltage U_a to the firing voltage FV, the plasma is ignited and the appearance of the 'Lissajous' figure is used as an unambiguous indicator for a breakdown. The exact value of FV was calculated according to the formula

$$FV = \frac{0.5C_d}{C_g + 0.5C_d} U_s + \frac{C_r}{C_d} U_r \quad , \tag{3}$$

where C_d is the capacitance of the dielectric layer, C_g is the capacitance of the gas gap, U_s and U_r are the voltages evaluated from the Lissajous figures (see the Figure 7) [9]. U_s is the instant value of the applied voltage at the moment of the discharge ignition. U_r is the voltage drop on C_r , caused by a charge transferred over the gas gap. The first addend in the right hand side of the formula is the voltage drop on the gas gap, caused by the applied voltage U_a at the moment of the discharge ignition. The second addend gives the voltage drop on the gas gap, caused by the charges accumulated on the surface of the dielectric layer via gas discharge. The sum of these voltage drops, FV, is equal to the breakdown voltage of the gas gap between the two samples having a certain secondary electron emission coefficient γ of the surface layers. Formula (3) is approximate, but holds well if $C_d << C_r$, and if the stray capacitance $C_{stray,}$ caused by all the surrounding capacitances (cables and edge effects) in parallel with the cell, is small as compared to C_r. In our case, C_{stray}=0.5 pF, C_g=3.71pF ±10%, C_d=180 pF ±20%, and C_r=5690 pF±5%. From these values the methodical errors can be estimated to be less than 0.1% and the use of Formula (3) is well justified. Some additional details for the interpretation of the Lissajous figures can be found in [10]. The experimental uncertainty of FV, as estimated on the basis of Formula (3), had an approximate value of 6 V.

5. MODIFICATION OF MAGNESIUM OXIDE STRUCTURE AND DEFECTS

5.1 Luminescence properties of laser-deposited MgO films

In order to investigate the intrinsic defects of laser-deposited MgO thin films and the possible influence of film thickness on the luminescence properties a series of MgO films with varying thicknesses (35 – 127) were grown. A plate cleaved from high-quality MgO single crystals grown by the arc-fusion method was used as a target. Films with different thicknesses were grown on Si substrates by varying the number of laser pulses. Deposition conditions were chosen as follows: laser pulse energy density on the target 7 J/cm^2, repetition rate of laser 10 Hz, substrate temperature 580 ^{o}C, and oxygen pressure in the chamber 0.2 Pa. Table 1 summarizes the results of structural analysis. The films were smooth with densities close to the theoretical MgO value (3.58 g/cm^3). According to XRD analysis, the films contained a cubic MgO crystal phase.

Table 1. Properties of MgO films evaluated by the XRR method.

Sample	Number of laser pulses	Film thickness nm	Film density g/cm^3	Film roughness nm
110	25, 000	127	3.40	0.8
112	17, 000	79	3.57	0.6
111	12, 500	55	3.46	0.6
113	9, 000	35	3.50	1.2

In order to investigate the properties of the electronic excitations of the films, cathodoluminescence (CL) studies and photoluminescence (PL) spectroscopy were performed. Figure 8a presents the CL spectrum of a high-purity MgO crystal at 5 K, and panel (b) shows typical spectra recorded from thin MgO films at 5 K and 293 K. The spectrum of the single crystal and films share similar features: they both have the edge emission of a large radius exciton peak at 7.65 eV and both have a broad emission band arising from the luminescence of F and F$^+$ centers. Thus, both samples contain anion vacancies. The major difference between the CL spectra of the studied PLD films and MgO single crystals is the absence of emission from V-type centers (bands in the region of 4–6 eV). According to reference [11], the CL emission peak at 5.3 eV depends strongly on the thickness of the electron-beam-deposited (EBD) MgO film – this emission band occurs only for the films thicker than at least 200 nm and is completely absent for 50 nm films. To investigate if this is also the case for our films, up to 500 nm thick MgO films were deposited and CL spectra recorded. For the 500 nm thick films, the emission from V-type centers was still missing from the spectrum. The crystallite sizes for 500 nm thick films were estimated from XRD graphs by using the Scherrer formula and were ranging between 16 – 23 nm for films grown at different conditions. Taking into account that the diffusion length of the free carriers reported in [12] for MgO was 220 nm, these results indicate that the most probable reason for the absence of luminescence from V-type centers is the small crystallite size, in which case the non–radiative recombination processes on the surfaces of the crystal grains play main role for our PLD films.

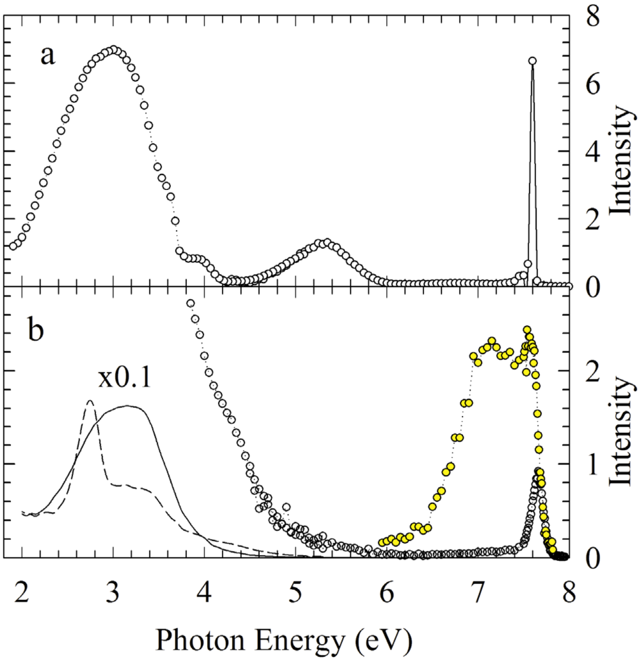

Figure 8. (a) Cathodoluminescence spectra of a high-purity MgO crystal at 5 K excited by 15 keV electrons. (b) Cathodoluminescence spectra of a MgO film (no. 111) recorded at 293 (yellow circles and solid line) and 5 K (open circles and dashed line). The energy of exciting electrons was 1 keV and the beam current 1 μA. The intensity in the low-energy part of both spectra at 293 K is scaled in order to visualize the high-energy part in more detail (the absolute value of intensity for VUV emission at 293 K is approximately 10 times smaller than that at 5 K).

5.2 Modification of structure

5.2.1 General considerations – role of structure

During the last decade, several reports have addressed the dependence of the electron emission coefficient or the firing voltage from the density, crystallinity or surface morphology (roughness) of films [13–17]. There are also a number of reports that describe the improvement of protective layer properties by modification its structure when ZnO, SiO_2, ZrO_2, CaO, Y_2O_3, Al_2O_3 or TiO_2 compounds have been added as dopants into MgO deposition targets [18–22]. By modifying the surface structure or its composition one can enhance the electron emission coefficient, which results in a reduced discharge voltage and a lower power consumption of the device. Typically, MgO protective layers have been prepared by the electron beam deposition (EBD) method [18–22], however, the reactive sputtering [23] and the ion beam-assisted technique [13, 14] have also been used. Although several studies have been dedicated to the pulsed laser deposition (PLD) of MgO films [24–27], there are no reports about a direct investigation of the properties of discharge cells with PLD-prepared pure or doped MgO films. At the same time, the PLD could be very versatile for the systematic studies of discharge cell coatings, allowing an easy change of deposition parameters, doping or combinatorial growth [28]. The characterization of the relations between the structural properties of PLD-made MgO thin films and the discharge characteristics of the cells is the primary objective of the present chapter.

5.2.2 Experimental

In this part of the work, 220–230 nm thick MgO films were deposited by the PLD method on fused silica substrates for a structural characterization and on special substrates for firing voltage measurements (see Figure 4). The cleaved high-quality MgO single crystals grown by the arc-fusion method [29] from a high-purity MgO powder (Alfa Aesar, 99.999%) were used as targets. Two main PLD deposition parameters were varied: the substrate temperature between 260 and 600 °C and the oxygen pressure in the chamber between 0.02 and 5 Pa. The laser pulse energy density on the target (~7 J/cm^2), the repetition rate of laser pulses (10 Hz), and the distance between the substrate and the target (7.5 cm) were held constant for all depositions. A typical film growth rate was 83 and 56 pm/s at 0.36 and 5 Pa deposition pressure, respectively.

5.2.3 Results and discussion

The FV as a function of the substrate temperature during the MgO film growth is presented in Figure 9. As one can see, FV generally decreases with increasing substrate temperature but the exact form of dependencies has different character for different oxygen pressures during the growth. Whereas a linear decrease of FV with substrate temperature is observed for the films grown at 5 Pa (Figure

9b), a more complex dependence is observed for the films grown at 0.36 Pa (Figure 9a). The data of XRD, XRR and AFM analysis made on the films grown at different substrate temperatures and oxygen pressures are collected in Table 2. From the data presented in Figure 9b and in Table 2 it can be concluded that there is a linear dependence between the FV and the density of the films grown at 5 Pa oxygen pressure (Figure 10). Note that the films grown at this oxygen pressure were XRD-amorphous, except for the film grown at the highest temperature, 600 °C. The crystallization was clearly inhibited at a higher O_2 pressure.

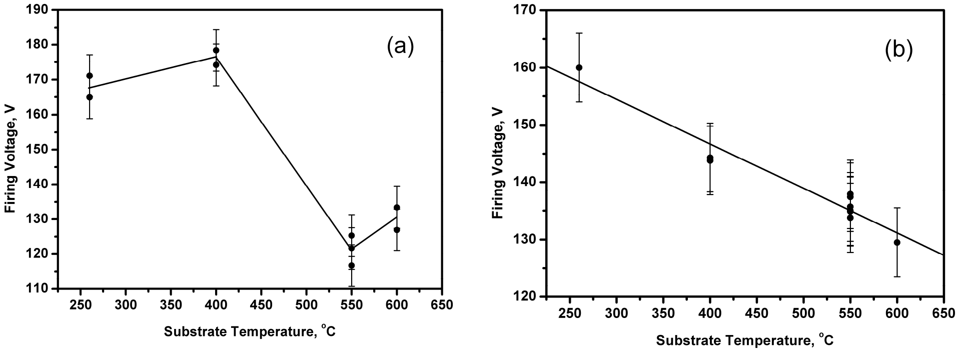

Figure 9. FV dependence on MgO film deposition conditions: on the substrate temperature at O_2 pressure of 0.36 Pa (a), and at O_2 pressure of 5 Pa (b).

Table 2. XRD, XRR and AFM analysis results for the MgO films grown at different O2 pressures and substrate temperatures.

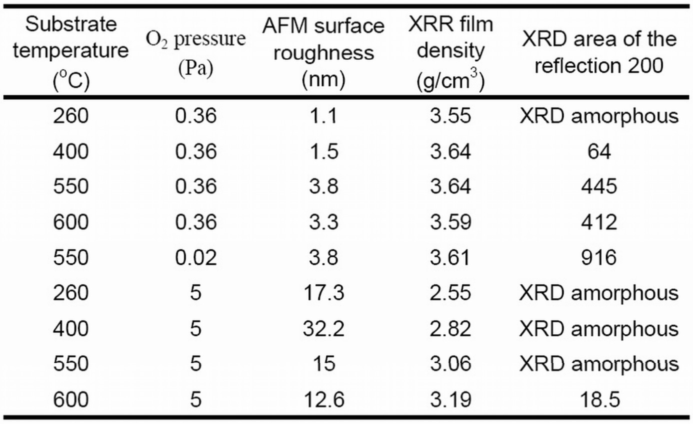

Substrate temperature (°C)	O_2 pressure (Pa)	AFM surface roughness (nm)	XRR film density (g/cm^3)	XRD area of the reflection 200
260	0.36	1.1	3.55	XRD amorphous
400	0.36	1.5	3.64	64
550	0.36	3.8	3.64	445
600	0.36	3.3	3.59	412
550	0.02	3.8	3.61	916
260	5	17.3	2.55	XRD amorphous
400	5	32.2	2.82	XRD amorphous
550	5	15	3.06	XRD amorphous
600	5	12.6	3.19	18.5

The films grown at a lower O_2 pressure (0.36 Pa) showed much higher crystallinity (see the data in Table 2, last column). . The diffractograms of these films grown at temperatures between 400 and 600 °C showed a MgO 200 diffraction peak and only the film grown at the lowest temperature (260 °C) was completely XRD-amorphous. The densities of all the films grown at 0.36 Pa coincided with a theoretical value for MgO (3.58 g/cm^3). From Figure 9a and Table 2 it can be concluded that the drop of FV values between 400 and 550 °C can be associated with the significant increase of crystallinity within this temperature interval.

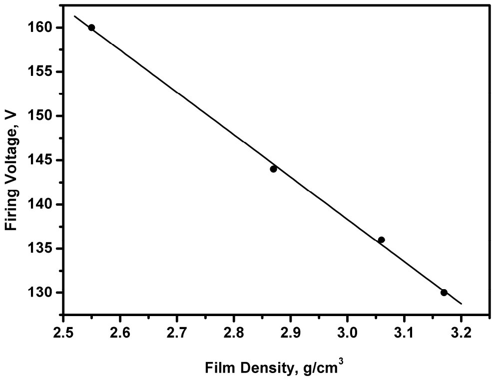

Figure 10. FV dependence on density for MgO films deposited at 5 Pa O_2 pressure.

A minimal FV value of ~120 V was obtained at 550 °C substrate temperature and O_2 pressure < 1 Pa. At these conditions films with a high crystallinity and density were obtained.

One may conclude that the high density and degree of crystallinity are generally required for having low FV values. However, a closer look at the data reveals also the role of surface roughness on the FV values. When comparing the samples grown at 400 °C substrate temperature and the pressures of 0.36 and 5 Pa, then it becomes evident that even though the sample grown at a lower pressure is (partly) crystalline and the one grown at a higher pressure is completely XRD-amorphous, the FV of the amorphous (and less dense) sample has a substantially lower FV value (Figures 9a and b). Note that the sample with a lower FV has a 20 times higher surface roughness value (Table 2). This example shows that, besides the fact that crystallinity and density are playing a significant role in FV, it is also influenced by the surface roughness. This conclusion can be further confirmed by the case that the films grown at 550 °C and 5 Pa, which are XRD-amorphous, show high roughness and a relatively low FV.

The film roughness (or surface morphology) is among the discussed factors that influence the discharge properties. However, the results concerning the FV dependence on the film roughness are not fully consistent [14,17,23,30]. Yasui et al. [17] have found that FV is decreased with the decreasing roughness of the films, while in the work of Park et al. [23] a sample with the highest roughness had the lowest FV. In references [14,30] the authors have found that the surface roughness has no considerable effect on the FV of MgO films. In our study, there are clearly two different cases concerning the dependence of the FV on the surface morphology. Let us compare the films grown between 400 and 600 °C at two different oxygen pressures. For the films grown at 5 Pa, one can observe a similar correlation to the one in reference [17] – the lower roughness results in a smaller FV, however, for the crystalline films grown at 0.36 Pa one obtains an opposite correlation between FV and the surface roughness – the higher the roughness is, the lower is the value of FV.

Our study reveals the fact that the correspondence between the investigated structural parameters (density, surface morphology, and crystallinity) and the FV or γ of the MgO film has a rather complex character. Although the high crystallinity and the density of films were the major factors resulting in low FV values, it was observed, in addition, that an increased surface roughness also contributed to the reduction of FV.

5.3 Modification of defects – hydrogen doping of MgO

5.3.1 General considerations – role of defects

By using additives to modify the morphological structure or the energy level structure of a MgO protective film, one can enhance the electron emission coefficient, which results in a reduced discharge voltage and a lower power consumption of the device. There are recent reports about the improvement of the discharge properties, namely the discharge delay time, of a MgO layer by introducing hydrogen-containing defects into the crystal lattice of the film [11, 31, 32]. A shorter discharge delay time allows an improving of the dynamic range of the gray scale and it also enables to simplify the principle of the operation of PDPs [11, 33]. In general, to a greater or lesser extent all oxide crystals contain some hydrogen, which enters the host lattice during the crystal growth. Most of the hydrogen is stored in three basic forms: OH^-, H_2 and $[H^-]^+$ [34] (Figure 11). Hydride ion H^- consists of a proton with two electrons. When H^- is substituting O^{2-} ions, it forms a so-called $[H^-]^+$ center which has a net positive charge [35]. As it is positively charged with respect to the lattice, it can trap another electron. $[H^-]^+$ centers act as a shallow (0.56 eV) [36] electron trap and can supply exoelectrons to reduce the discharge delay time of the discharge cell. The exoelectron is the electron emitted into the discharge space from the MgO layer through various relaxation processes and it can serve as a priming species for gas discharge events in a cell [11, 33].

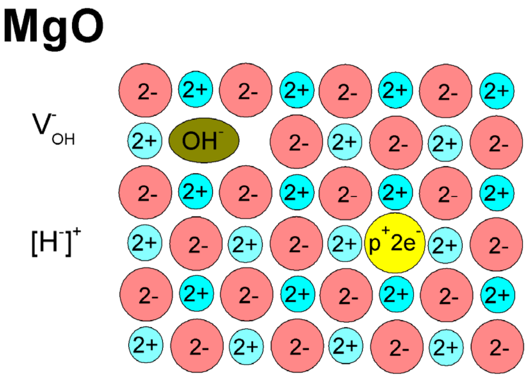

Figure 11. Schematics of hydrogen-related defects in a MgO crystal.

A lowering of the discharge voltage, when H_2 gas was added into deposition atmosphere of MgO coating, has also been reported in some references [31, 37]. Previously, hydrogen doping in the MgO protective coating was achieved by adding hydrogen gas into the chamber atmosphere during the electron beam deposition, the radio frequency magnetron sputtering or the ion plating deposition process of the MgO film. This can also be done by a post-treatment of the deposited MgO film, e.g. by hydrogen containing plasma [11]. In this work, hydrogen-doped MgO films were prepared by a pulsed laser deposition method by using the arc-fusion-grown MgO single crystals as ablation targets. These crystals almost always have regions, appearing milky (or cloudy) to the unaided eye, that are filled with small bubbles of hydrogen gas at a high (~40 MPa) pressure [38]. Such crystals have also clear regions, which do not have hydrogen-filled cavities and contain substantially less hydroxyl complexes (OH^-) than milky regions. In this study, the effect of hydrogen doping on the FV value and on the FV frequency dependence was investigated by using crystal targets with a high hydrogen content as compared to the targets with a negligible hydrogen concentration. The effect of a small amount of N_2 gas in a standard discharge mixture on the FV frequency dependence was also studied.

It has to be noted that there have been some previous reports about a hydrogen addition of MgO films for PDP application [31, 37] but the results of the present work are the first ones that clearly indicate the creation of hydrogen-related defect states. The dependence of the firing voltage on the AC frequency of the hydrogen-doped MgO films is also studied for the first time in this work.

5.3.2 Experimental

MgO films were deposited by the PLD method on two types of substrates: (a) Si(1 0 0) substrates for low-temperature thermoluminescence measurements; (b) special substrates (Figure 4) for FV measurements. The 220–230nm and 500nm thick films were deposited for FV and luminescence measurements, respectively. The plates cleaved from high-quality MgO single crystals grown by the arc fusion method from powder, were used as targets. The MgO powders used in the growth procedure were >99.9% purity. Two types of crystals were used: (a) crystal slabs cleaved from the regions of high H_2 content – milky targets, and (b) clear targets cleaved from the regions where the hydrogen concentration is negligible (Figure 12). The deposition conditions of the MgO films were as follows: laser wavelength 248 nm, the laser pulse energy density on the target 7 or 10 J/cm^2, the repetition rate of laser 10 Hz, the substrate temperature 550 ^{o}C, the distance between the substrate and the target 7.5 cm, and oxygen pressure in the chamber 0.36 or 5 Pa.

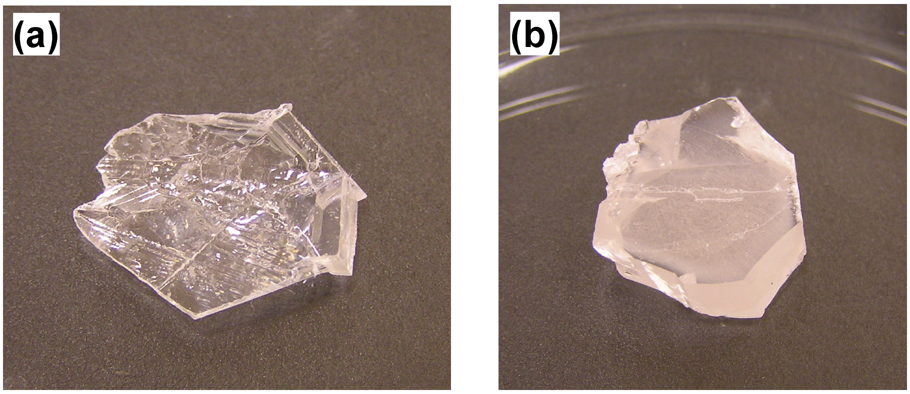

Figure 12. “Clear” (a) and “milky” (b) single-crystal PLD targets used for the deposition of reference films and H-doped MgO films, respectively.

5.3.3 Results and discussion

The thermoluminescence glow curves of the MgO films deposited from clear (further denoted as sample “clear”) and milky (sample “milky”) crystals are shown in Figure 13. The TL curves have two dominating peaks centered at 88 and 241 K, respectively. After the fitting procedure, the activation energies calculated for the peaks at 88 and 241K were 0.051 and 0.31 eV, respectively. According to reference [34], these peaks can be attributed to two types of electron traps involving hydrogen: H^{2-} (low- temperature peak) centers and $[H_x^-]^0$ (high-temperature peak) centers. TL results when electrons are released from these electron traps and recombine with F^+ centers followed by radiative de-excitation:

$[H_x^-]^0 + kT \rightarrow [H_x^-]^+ + e$
and $H^{2-} + kT \rightarrow H^- + e$
$e + F^+ \rightarrow F^* \rightarrow F + h\upsilon$ (i.e. TL)

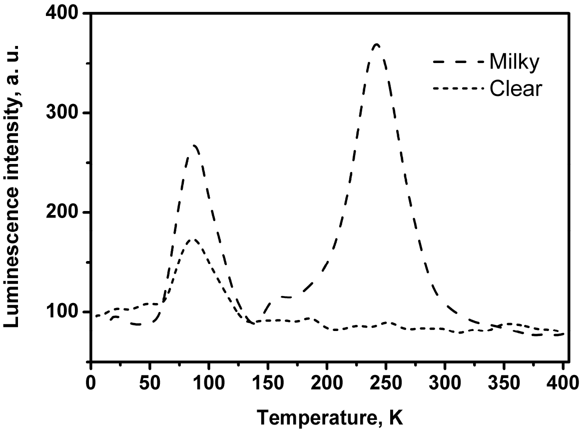

Figure 13. Integral TL spectra (185–650 nm) of the films deposited from milky and clear targets after e-beam irradiation at 6K.

The FV frequency dependences measured in a standard gas mixture (Ne–10% Xe) and an N_2-modified gas mixture (Ne–10% Xe–0.05%N2) are depicted in Figure 14. It can be seen from the figure that in a standard gas mixture, the FVs of the "clear" sample fall between 203 and 219 V, and are shifted to about 10 V higher values if measured in a N_2- modified mixture. Similar influence of N_2-modified gas mixture on FVs is reported in reference [39] – the FVs of the samples were 4% higher in a 0.2% N_2-modified gas mixture as compared to an unmodified mixture (He + 70% Ne + 4% Xe). In [39], it was proposed that the negative effect of N_2 arises due to the formation of the negative ions N_2^-, leading to the decreased electron temperature of plasma, which in consequence, influences adversely γ value and results in higher FV values.

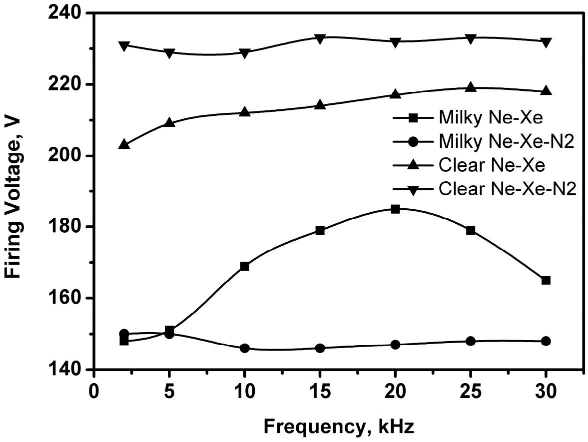

Figure 14. Firing voltage frequency dependence of the thin films deposited from milky and clear MgO targets.

The FV values of the “milky” sample are considerably lower than those of the “clear” sample (Figure 14). Depending on the AC frequency, the FVs are up to 55 V lower. Similar results have been obtained in reference [31], where the characteristics of the electron-beam-deposited MgO film were investigated at a constant AC frequency of 2 kHz. In that work, the MgO film was deposited with H_2 atmosphere in the deposition chamber. The study showed that the FVs of the film prepared under H_2 flow was at most 34V lower than those of the reference sample.

The FVs of our “milky” sample were considerably influenced by N_2 additive in the discharge gas mixture – the frequency dependence of FVs practically disappeared. For instance, the FV value at 20 kHz is lowered from 185 V to 147 V. The lowering of FV values in a standard gas mixture for a hydrogen-doped sample can be explained by considering the effect of the doping on the electron energy levels in the film. The effect of the F-type center density in MgO on FV was investigated experimentally and calculated theoretically in references [4, 40]. The adding of the energy levels of F and F^+ centers into the MgO band gap resulted in the lowered FV and even more important changes in γ value for Xe^+ ions, being different from zero (the theoretical γ due to ion impact is determined to be 0.29 for Ne^+ and 0 for Xe^+ ions [1]). It is easier to emit an electron from the high-energy defect level than from the valence band – the parameter G (Formula 2) is larger for the processes 1 + 4 and 2 + 4 than for the processes 1 +3 and 2 + 3 in Figure 15. Remember that γ is larger with the increasing of parameter G.

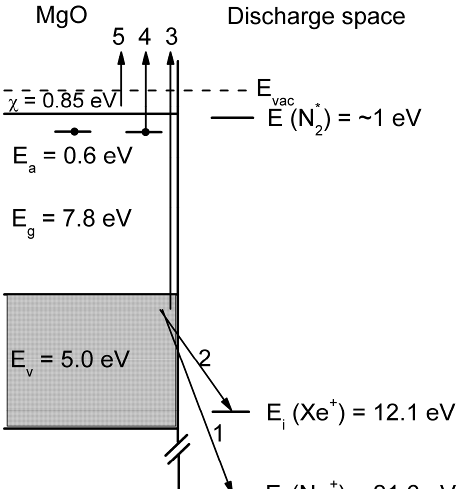

Figure 15. A simplified energy level diagram showing the involved MgO, Ne, Xe and N_2 energy levels relative to the vacuum level and possible Auger emission processes. For detailed explanation see the corresponding text.

The FV frequency dependence of the “milky” sample can interpreted as follows: one can estimate the time τ for the electron to be exited from a trap with the electron activation energy of E_a by using the following formula: $\tau = p_0^{-1}\exp(E_a/k_BT)$, where p_0 is a frequency factor or attempt frequency, T is temperature and k_B is the Boltzmann constant. If we use T = 300K (RT) and $p_0 = 3\times109\ s^{-1}$ as in work [33], then we get τ = 0.06 ms. At low frequencies, the AC half period time is much longer than τ and the electrons in traps have enough time to be excited to the conduction band. It is possible that the decreased FV at lower frequencies is due to the increased γ values for Ne^+ and Xe^+ ions if the electrons that participate in Auger process have higher energies (processes 1 + 5 and 2 + 5 in Figure 15).

The influence of N_2 gas in the discharge mixture (disappearance of the frequency dependence of FVs for the “milky” sample) can be attributed to the energy transfer between the electron traps at the surface and N_2 molecules in the discharge gas. N_2 molecules are reported to have a long-lived vibrationally excited metastable state, having the energies of about 1 eV [41] (see Figure 15). Therefore, energy transfer processes may take place between the shallow electron traps in MgO and vibrationally excited nitrogen molecules, as the addition of N_2 can provide a large amount of vibrationally excited metastable nitrogen molecules in the discharge gas. This increases the number of electrons in the conduction band and the probability for electron emission involving energetic Ne^+ and Xe^+ ions (processes 1 + 5 and 2 + 5 in Figure 15).

6. POSSIBLE REPLACEMENT MATERIALS OF MAGNESIUM OXIDE – BARIUM TERNARY OXIDES

6.1. General considerations

If the electron emission is determined primarily by E_g and χ,, the lowering of the energy consumption of PDPs can be achieved by replacing MgO with a dielectric with a smaller χ value, but also hopefully with a reduced energy gap E_g. The best-known competitors for MgO are CaO, SrO, BaO (χ = 0.6 eV [42]) and their mixtures, which are widely exploited in multi-component oxide thermo cathodes. The latter devices have been in use for more than half a century, and a vast comprehensive literature has been accumulated over the years (see, e.g. monographs [43, 44], and a recent review [45]). However, the direct application of oxide thermionic cathode materials in PDPs is not straightforward. Along with obvious advantages, there are complications, the most important of which is the highly hygroscopic nature of alkaline-earth oxides in the form of $(Ba_xSr_yCa_z)O$. To overcome this problem, we chose a thermochemically stable Ba containing dielectric materials, barium gallate $BaGa_2O_4$ and barium yttrate BaY_2O_4, in particular, to investigate them for PDP applications. The precise values of E_g of these compounds are not known, however, there are estimates available that are based on the analysis of the luminescence excitation spectra recorded for various phosphor materials – E_g ~5.6 eV for BaY_2O_4 : Pb [46] and E_g ~5.0–5.5 eV for $MgGa_2O_4$: Mn, $ZnGa_2O_4$:Mn and $CaGa_2O_4$:Mn [47]. We can expect that the band gap energies for the selected ternary compounds are significantly lower than that of MgO (Eg = 7.8 eV) [48]. However, due to experimental difficulties, the electron affinity values of $BaGa_2O_4$ and BaY_2O_4 compounds (and many others) are not known. We chose a direct way to investigate the FV values and other characteristics of the selected compounds and to compare these with the corresponding data for MgO.

6.2. Experimental

An undoped BaY_2O_4 powder was prepared by using a thermal decomposition of a mixture of barium and yttrium nitrates (99.9%), by a stepwise heating up to 900 °C. For preparing a pure $BaGa_2O_4$, the starting materials were $BaCO_3$ (99.999%) and Ga_2O_3 (99.997%), which were mixed, pressed into pellets, and annealed at 1200 °C for 18 h. After that the obtained mixtures were ground, thoroughly mixed and pressed again. The final sintering of both compounds was carried out at 1300 °C for 5 h in an oxygen flow. The films were deposited onto special substrates for FV measurements or onto Si(100) and Pt(111)/Ti/SiO_2/Si substrates for a structural characterization. In all depositions the repetition rate of laser pulses was 10Hz and the energy density of the laser pulse on the target was in the range of 1.5–2.5 J cm^{-2}. The substrate temperature was varied between 260 and 850 °C, and the oxygen pressure in the chamber was varied between 0.04 and 10 Pa. The thicknesses of all films, as determined from the optical reflectance, were between 200 and 500 nm.

6.3 Results and discussion

According to an XRD analysis, the films of both materials deposited at relatively low temperatures (<600 °C), were amorphous. $BaGa_2O_4$ was investigated more extensively, since the literature data predicted more promising energetic properties of this compound for PDP applications. The XRD diffractograms of $BaGa_2O_4$ films deposited on Si substrates at two different temperatures are depicted in Figure 16. The data show that the film grown at 620 °C is completely XRD-amorphous, but the pattern of the film grown at 750 °C has several diffraction peaks, which indicate that the film contains a crystalline $BaGa_2O_4$, which shows a preferred orientation (0 0 1).

According to the electron probe microanalysis (EPMA) and x-ray photoelectron spectroscopy (XPS) data, the films grown at the oxygen pressures of or above 1 Pa were stoichiometric – the Ga/Ba ratio was determined to be 1.9. At lower oxygen pressures a deficit of Ga was observed – for the films grown at the lowest oxygen pressure, 0.04 Pa, the Ga/Ba ratio was only 1.6. It was also observed that a considerable Ga deficit developed in the surface layers of the films stored under an ambient atmosphere, which indicates a hygroscopic or an unstable nature of the material.

The samples prepared by PLD for FV measurements were grown at 250 °C and at 1 Pa (Ba-yttrate) or 5 Pa (Ba-gallate) oxygen pressure, which resulted in the films of an amorphous structure. A higher oxygen pressure during the deposition of the latter compound resulted in the films with a better stoichiometry because of a smaller loss of Ga. The properties of the materials can be summarized as follows: the films were amorphous and had but small non-stoichiometric consistency with respect to Ba.

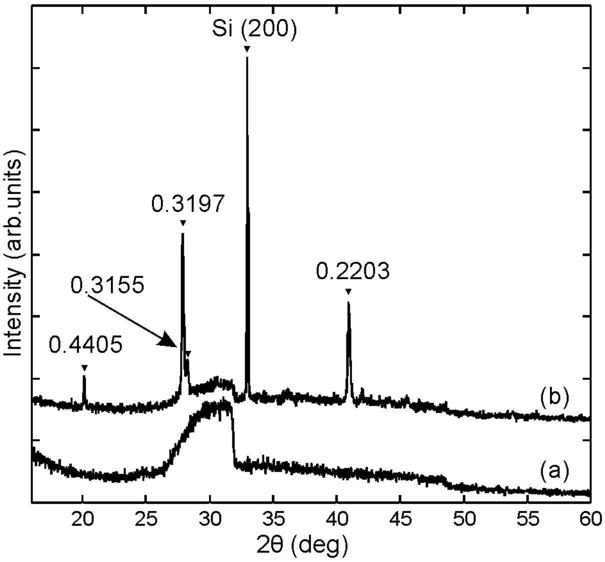

Figure 16. XRD pattern (Cu Kα radiation) of the Ba-gallate samples grown at 620°C (a) and at 750°C (b). The broad reflection at 30° and the narrow one at 33° originate from the Si substrate. The corresponding lattice distances (d, nm) for the reflections from the film are displayed near the peaks.

For the compounds investigated in this work, the FV values, being equal to 210V for BaY_2O_4 and 257 V for $BaGa_2O_4$, are much higher than for the standard MgO films – as presented above in section 5.1, completely XRD-amorphous MgO films had FV values between 135 and 180 V. The question is, which energetic parameter, Eg or χ, plays a major role in such results obtained for ternary complex oxides? For a more precise determination of the E_g values of the substances under investigation, the luminescence and excitation spectra for observable emissions of PLD targets were recorded in a wide range of incident photon energies in the VUV region. Figure 17 shows the emission spectrum (symbols) and excitation spectra for two emission bands recorded at 2.58 eV and 3.94 eV (line and filled symbols, respectively) in $BaGa_2O_4$ at 9K. In the emission spectrum, two partially overlapping bands with peaks at 2.95 and 3.8 eV are observed. The ~2.95 eV band in $BaGa_2O_4$ and low intensity ~3.2 eV emission in BaY_2O_4 (which contributes to the main 4.1 eV band as a tail) are ascribed to the self-activated luminescence centers. The short wavelength emissions at ~3.8 and ~4.1 eV are assigned to the radiative decay of excitons in Ba-gallate and Ba-yttrate, respectively. The enhancement of the long-wavelength emission at 2.95 eV in $BaGa_2O_4$ shows the presence of defects due to oxygen deficiency, reducing the intensity of the excitonic band at 3.8 eV, which is a natural result of a competition between different luminescence centers. Our luminescence data on BaY_2O_4 with the dominating excitonic emission at 4.1 eV indicate a less defective nature of this material. Taking into account the results of [46, 47] and the analysis of our experimental data, the estimates for the energy gap E_g for $BaGa_2O_4$ and BaY_2O_4 are ~5.8 eV and ~6.2 eV, respectively. Analogously, the luminescence maxima of the excitonic emission band in these systems exhibit a similar shift, ~3.8 eV and ~4.1 eV, respectively.

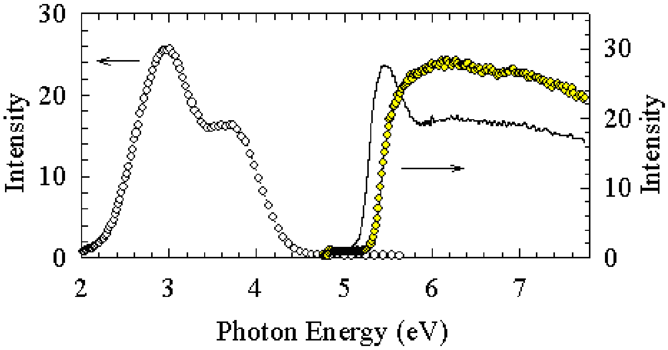

Figure 17. Emission (symbols) and excitation spectra of 2.58 eV (line) and 3.94 eV (filled symbols) emission of $BaGa_2O_4$ ceramics at T = 9K. Exciting photon energy was 6.2 eV.

A comparison of the energy gap values of BaY_2O_4 (6.2 eV), $BaGa_2O_4$ (5.8 eV) and that of MgO (7.8 eV) allows a conclusion that the cause of the sharp increase in the FV (210 and 257 V) with respect to MgO (<180 V) is mostly due to the high electron affinity χ of the ternary oxides compared to MgO's (χ = 0.85 eV), such as the case of ZrO_2 [49]. Even though we did not directly record χ values, our results on the FV let us establish the relation χ (MgO) < χ (BaY_2O_4) < χ ($BaGa_2O_4$). Reference [50] reports χ values of 2 eV for Y_2O_3 and Ga_2O_3 has χ = 3.65 eV according to [51]. These χ values are in good correlation with the relationship obtained for the ternary oxides studied by us.

However, it has to be noted that behavior of the material in an operating PDP cell and its FV, is clearly not determined only by the sum of E_g and χ. The secondary electron emission coefficient γ depends also on other factors. For example, on the existence of intrinsic or extrinsic defects having suitable electron energy levels to favor the dynamical processes taking place during the work of the cell and involving charge accumulation and transport at the surface of the dielectric coating. The energy needed for the desorption of the accumulated electrons may be significantly lower than the energy necessary for an electron emission from a non-activated surface under zero field conditions in vacuum.

7. CONCLUSIONS

In this thesis work, the materials for the protective coatings of plasma display panels (PDP) were studied with the aim to improve the discharging properties of coatings, which are essential for lowering the power consumption and cost-effectiveness of PDPs. Among the studied materials were undoped and doped MgO, $BaGa_2O_4$ and BaY_2O_4 . The pulsed laser deposition (PLD) method was used for synthesizing the films. Relations between the structural properties of the grown films and the laser deposition conditions were investigated. The firing voltage (FV) measurements and the luminescence measurements of selected samples were performed.

The luminescence spectra of laser-deposited MgO thin films contained the bands of color centers (F and F^+) in the visible region as well as those of large radius excitons in the VUV region. The emission band from V_M-type centers, which was present in the spectra of MgO single-crystal targets, was missing for all MgO films. This is probably caused by a surface (radiationless) recombination in thin films, where the mean crystallite size (<25 nm) is small in comparison with the diffusion length of free charge carriers.

The optimal deposition conditions of MgO thin films on amorphous substrates were found for obtaining a minimal firing voltage for the growth temperatures up to 600 °C. The minimal FV values of 120 V were obtained on the samples grown at 550 °C and $p < 1$ Pa oxygen pressure. Films with good crystallinity and high density (close to theoretical MgO density of 3.58 g/cm^3) were obtained at optimal conditions. The densities of the films grown at a higher pressure (5 Pa) increased with the rising growth temperature and were closely correlated with the FVs – denser MgO films had lower FV values. Although the density and the crystallinity of the films were the main factors influencing the FV values, it was also observed that the high surface roughness of the films favored the achieving of low FVs.

Milky MgO single-crystal slabs that contained hydrogen gas bubbles at high pressure were used as PLD targets for doping MgO films with hydrogen impurities. Thermoluminescence measurements indicated that the film deposited from a milky target contained electron traps with the activation energy of 0.31 eV, while these traps were absent for the films grown from the targets not containing hydrogen-filled cavities. According to previously published works, these traps can be assigned to H^- filled oxygen vacancies in the MgO crystal lattice. The sample deposited from a milky crystal had up to 55 V (27%) lower FVs than the ones grown from a clear target. In the case of films with hydrogen traps, the addition of N_2 gas to the standard discharge mixture lead to the lowering of FVs at higher AC frequencies (up to 37 V or 20% at 20 kHz).

Two barium ternary oxides, BaY_2O_4 and $BaGa_2O_4$, were considered as a plasma display protective coating material candidates. The luminescence properties of these materials and the structure of the films were studied. The bandgap energies of BaY_2O_4 and $BaGa_2O_4$, estimated from the luminescence excitation spectra, were 6.2 and 5.8 eV, respectively. The FV values of BaY_2O_4 (210 V) and $BaGa_2O_4$ (257 V) were considerably higher as compared to the FVs of MgO films (<180 V).

SUMMARY IN ESTONIAN

Magneesium oksiidi ja baariumi kolmikoksiidide õhukeste kilede impulss-lasersadestamine plasmakuvarite kaitsekihtide rakenduseks

Antud doktoritöös uuriti plasmaekraanide kaitsekihtide materjale ühe plasmaekraanide olulisima parameetri, süttimispinge, seisukohast. Plasmaekraanid koosnevad tuhandtetest gaaslahendusrakkudest ja ekraanide energiatarve ja maksumus on otseselt seotud rakkudes tekitatava gaaslahenduse süttimispingega – mida madalam süttimispinge, seda madalam energiatarve ja seda vähem maksavad ekraanis sisalduvad elektroonikakomponendid. Sünteesitud materjalide süttimispingete mõõtmiseks sadestati uuritavast materjalist kiled spetsiaalsetele alektroodalustele ja mõõdeti kahest vastakuti asetatud alusest koosneva testraku süttimispinge. Õhukeste kilede sadesamiseks kasutati impulss-lasersadestuse seadet. Töös käsitletud materjalideks olid $BaGa_2O_4$, BaY_2O_4 ning puhas ja dopeeritud MgO. Magneesium oksiidi – mis on ka hetkel plasmaekraanis tööstuslikult kasutatav kaitsekihi materjal – korral uuriti sadestustingimuste mõju kasvanud kilede struktuurile ning kilede struktuuri ja dopeerimise mõju gaaslahendusomadustele. Uuriti ka kahe potentsiaalse kaitsekihi asendusmaterjali, $BaGa_2O_4$ ja BaY_2O_4, kilede struktuuri ja gaaslahendusomadusi.

MgO õhukeste kilede katoodluminestsentsi spektrid sisaldasid ribasid spektri nähtavas osas, mida võib omistada värvitsentritele (F ja F^+) ja ribasid vaakumultravioletses osas, mida saab omistada suure raadiusega eksitonide kiirgusele. V_M-tüüpi tsentrite kiirgusriba, mis oli selgelt nähtav MgO monokristallide spektris, puudus õhukeste kilede spektrites. See on tõenäoliselt tingitud vabade laengukandjate kiirguseta rekombinatsioonist kristalliitide piirpindadel, kuna kristalliitide suurused (<25 nm) on oluliselt väiksemad võrreldes laengukandjate vaba tee pikkusega.

Leiti optimaalsed sadestustingimused amorfsetele alustele sadestatud MgO kilede süttimispinge minimeerimiseks. Minimaalne süttimispinge 120 V saadi proovidel, mis olid kasvatatud aluse temperatuuril 550 ^oC ja hapnikurõhul $p < 1$ Pa. Optimaalsetel tingimustel kasvasid suure tihedusega (MgO teoreetilisele tihedusele 3.58 g/cm^3 lähedase tihedusega) kristallilised MgO kiled. Kõrgemal hapnikurõhul (5 Pa) kasvatatud kilede tihedused kasvasid koos kasvatustemperatuuri tõusuga. Nende kilede tihedused olid heas korrelatsioonis süttimispingega – mida suurem oli kilede tihedus, seda väiksem oli süttimispinge. Kuigi MgO kilede tihedus ja kristallilisus olid madala süttimispinge saavutamiseks olulisimad faktorid, selgus analüüsiandmetest, et ka kilede suur pinnakaredus soodustab madala süttimispinge saavutamist.

MgO õhukeste kilede vesinikuga dopeerimisel kasutati vesinikuallikana piimjaid (valgust hajutavaid) MgO monokristall-märklaudu, mis sisaldasid suure rõhu all olevaid vesinikumullikesi. Termoluminestsentsmõõtmised näitasid, et piimjast märklauast sadestatud MgO kiled sisaldasid 0.31 eV aktivatsioonienergiaga elektronide lõkse. Samas puudusid sellised lõksud MgO kiledel, mis olid sadestatud selgetest märklaudadest. Kirjandusest lähtuvalt võib need lõksud omistada H^- vesinikuiooniga täidetud hapnikuvakantsidele MgO kristallvõres. Piimjast märklauast sadestatud provide süttimispinged oli kuni 55 V (27%) madalamad kui võrdlusproovil. Vesinikulõkse sisaldava proovide korral mõjutas lämmastiku lisamine standardgaasisegule nende gaaslahendusomadusi – sõltuvalt vahelduvvoolu sagedusest langes süttimispinge kõrgematel sagedustel kuni 37 V (20%).

Kahte baariumi kolmikoksiidi, BaY_2O_4 ja $BaGa_2O_4$, uuriti lähtuvalt nende võimalikust kasutatavusest MgO asendusmaterjalidena plasmaekraanide kaitsekiledes. Uuriti nende materjalide luminestsentsomadusi ja neist sadestatud kilede struktuuriomadusi. Ergastusspektrite põhjal on hinnangulised BaY_2O_4 ja $BaGa_2O_4$ keelutsooni laiused vastavalt 6.2 ja 5.8 eV. Süttimispingete väärtusteks saadi antud materjalide korral 210 V (BaY_2O_4) ja 257 V ($BaGa_2O_4$), mis on oluliselt kõrgemad võrreldes MgO kiledel mõõdetud väärtustega (<180 V).

REFERENCES

[1] J.P. Boeuf, J. Phys. D: Appl. Phys. 36 (2003) R53–R79.

[2] T. Urade, T. Iemori, M. Osawa, N. Nakayama, I. Morita, IEEE Trans. Electron. Devices 23 (1976) 313–318.

[3] S. G. Ahn, S. H. Yoon, Y. S. Kim, Thin Solid Films 517 (2009) 4027–4030.

[4] Y. Motoyama, F. Sato, IEEE Trans. Plasma Sci. 34 (2006) 336–342.

[5] P. R. Willmott, J. R. Huber, Reviews of Modern Physics 72 (2000) 315–328.

[6] S. Bär, Crystalline, Rare – Earth -doped Sesquioxide PLD – Films on α – Alumina, CUVILLER VERLAG, Göttingen, 2004, p. 25–41.

[7] H. Mändar, J. Felsche, V. Mikli, T. Vajakas, J. Appl. Crystallogr. 32 (1999) 345.

[8] L.G. Parratt, Phys. Rev. 95 (1954) 359.

[9] P. K. Bachmann, V. van Elsbergen, D. U. Wiechert, G. Zhong, J. Robertson, Diamond Relat. Mater. 10 (2001) 809.

[10] Z. Falkenstein, J. J. Coogan, J. Phys. D Appl. Phys. 30 (1997) 817.

[11] H. Tolner, Invited Lecture, 41st PDP International Forum, Takamatsu, Japan, 10 December, 2005.

[12] M. Elango, J. Pruulmann, A.P. Zhurakovskii, Phys. Stat. Sol. (b) 115 (1983) 399.

[13] Z. N. Yu, J. W. Seo, S. J. Yu, D. X. Zheng, J. Sun, Surf. Coat. Technol. 162 (2002) 11.

[14] Y. Morimoto, Y. Tanaka, A. Ide-Ektessabi, Nucl. Instrum. Methods Phys. Res. Sect. B 249 (2006) 440.

[15] Z. N. Yu, J. W. Seo, D. X. Zheng, J. Sun, Surf. Coat. Technol. 163–164 (2003) 398.

[16] Y. H. Cheng, H. Kupfer, F. Richter, J. Appl. Phys. 94 (2003) 3627.

[17] N. Yasui, H. Nomura, A. Ide-Ektessabi, Thin Solid Films 447–448 (2004) 377.

[18] R. Kim, Y. Kim, J. W. Park, Vacuum 61 (2001) 37.

[19] H. K. Lee, W. J. Kim, S. J. Park, S. Y. Choi, Thin Solid Films 515 (2007) 5113.

[20] J. Cho, R. Kim, K.W. Lee, G.Y. Yeom, J.Y. Kim, J.W. Park, Thin Solid Films 350 (1999) 173.

[21] B. Guo, C. Liu, Z. Song, L. Liu, Y. Fan, X. Xia, J. Appl. Phys. 98 (2005) 043304.

[22] S. K. Ram, U. K. Barik, S. Sarkar, P. Biswas, V. Singh, H. K. Diwivedi, S. Kumar, Thin Solid Films 517 (2009) 6252–6255.

[23] C. H. Park, Y. K. Kim, S. H. Lee, W. G. Lee, Y. M. Sung, Thin Solid Films 366 (2000) 88.

[24] T. Chen, X. M. Li, S. Zhang, H. R. Zeng, J. Cryst. Growth 270 (2004) 553.

[25] T. J. Zhu, L. Lu, X. B. Zhao, Mater. Sci. Eng., B 129 (2006) 96.

[26] R. Hühne, C. Beyer, B. Holzapfel, C.G. Oertel, L. Schultz, W. Skrotzki, Cryst. Res. Technol. 35 (2000) 419.

[27] T. Susaki, S. Kumada, T. Katase, K. Matsuzaki, M. Miyakawa, H. Hosono, Appl. Phys. Express 2 (2009) 091403.

[28] R. Eason, Pulsed Laser Deposition of Thin Films, John Wiley & Sons, Inc., Hoboken, New Jersey, 2007.

[29] A. Maaroos, Trudy Inst. Fiz. Estonskoi SSR 53 (1982) 49.

[30] T. Nakano, T. Fujimoto, S. Baba, Vacuum 74 (2004) 595.

[31] K. H. Park, M. S. Ko, Y. S. Kim, Solid State Phenom. 124–126 (2007) 351–354.

[32] G. S. Lee, K.B. Kim, J. J. Kim, S. H. Sohn, J. Phys. D: Appl. Phys. 42 (2009) 105402.

[33] Y. S. Kim, S. H. Yoon, H. Yang, J. Appl. Phys. 107 (2010) 013303.

[34] R. Gonzalez, Y. Chen, J. Phys. Condens. Matter 14 (2002) R1143–R1173.

[35] V. M. Orera, Y. Chen, Phys. Rev. B (1987) 6120–6124.

[36] B. T. Jeffries, R. Gonzalez, Y. Chen, G. P. Summers, Phys. Rev. B 25 (1982) 2077–2080.

[37] M. Terauchi, J. Hashimoto, H. Nishitani, Y. Fukui, M. Okafuji, H. Yamashita, H. Hayata, T. Okuma, H. Yamanishi, M. Nishitani, M. Kitagawe, J. Soc. Inf. Disp. 16 (2008) 1195–1201.

[38] A. Briggs, J. Mater. Sci. 10 (1975) 729–736.

[39] J. H. Shin, C. H. Park, J. Korean Inst. Electric. Electr. Mater. Eng. 15 (2002) 909 913.

[40] Y. Motoyama, Y. Hirano, K. Ishii, Y. Murakami, F. Sato, J. Appl. Phys. 95 (2004) 8419–8424.

[41] Y. B. Golubovskii, V. A. Maiorov, J. F. Behnke, J. Phys. D: Appl. Phys. 35 (2002) 751–761.

[42] T. J. Vink, A. R. Balkenende, R. G. F. A. Verbeek, H. A. M. van Hal, S. T. de Zwart, Appl. Phys. Lett. 80 (2002) 2216–18.

[43] V. S. Fomenko, Handbook of Thermionic Properties. Electronic Work Functions and Richardson Constants of Elements and Compounds, New York: Plenum Press Data Division, 1966.

[44] B. P. Nikonov, Oxide Cathodes, Moscow: Energia, 1979 (in Russian).

[45] S. Yamamoto, Rep. Prog. Phys. 69 (2006) 181–232.

[46] T. I. Savikhina, I. A. Meriloo, Tr. Inst. Fiz. Akad. Nauk Est. SSR 49 (1979) 146–71 (in Russian).

[47] T. I. Savikhina, Tr. Inst. Fiz. Akad. Nauk Est. SSR 40 (1972) 24–52 (in Russian).

[48] E. Feldbach, I. Kuusmann, G. Zimmerer, J. Lumin. 24–25 (1981) 433–6.

[49] Y. T. Matulevich, M. S. Lee, J. H. Kim, J. S. Choi, S. K. Kim, S. S. Suh, D. S. Zang, J. Aarik, A. Aidla, M. Aints, J. Raud, M. Kirm, Appl. Phys. Lett. 88 (2006) 211504.

[50] P . Odier, J. P. Loup, J. Solid State Chem. 34 (1980) 107–19.

[51] J. Portier, G. Campet, A. Poquet, C. Marcel, M. A. Submarian, Int. J. Inorg. Mater. 3 (2001) 1039–43.

ACKNOWLEDGEMENTS

At first, I would like to thank all the people working at the Institute of Physics who have directly or indirectly contributed to this work.

I am very thankful to all my co-authors. Especially I would like to emphasize the support from Dr Marco Kirm, Dr Eduard Feldbach, Dr Tea Avarmaa and Dr Viktor Denks. Special thanks to Dr Jüri Raud for spending many hours by measuring the firing voltages of a countless number of samples I fabricated.

I am very thankful to Dr Yury Matulevich from Samsung SDI for being a helpful collaboration partner from the Samsung's side and for providing us with the information and the materials needed.

I would like to express my special thanks to my supervisor Dr Raivo Jaaniso for giving me the opportunity to work in his group and for his numerous consultations in scientific matters.

Special thanks to my colleague MSc Aare Floren, who is not among my co-authors, but whose help with resolving technical problems has been invaluable not only for the completion of this thesis work, but also for challenging technical matters in professional and private life.

I would like to thank my family for their support during my academic studies and sister Kaire for her encouragement in pursuing my PhD degree.

I am very thankful to Estonian Nanotechnology Competence Center for the possibility to participate in the gas-sensor project during my doctoral studies. This has been complementary financial support and experience in another research field during my studies.

This work was partly supported by Estonian Science Foundation grants nos. 6010 and 8306. Author wishes to acknowledge gratefully the support of the graduate school "Functional materials and processes" (at University of Tartu and Tallinn University of Technology) receiving funding from the European Social Fund under project 1.2.0401.09-0079 in Estonia.

PUBLICATIONS

CURRICULUM VITAE

General data

Name and surname: Margus Kodu
Date and place of birth: 16.12.1982, Antsla, Estonia
Citizenship: Estonian
Maritial status: unmarried, 1 child
Aaddress: Institute of Physics University of Tartu,
Riia 142, 51014 Tartu, Estonia
Phone: +372 737 4711, +372 5666 7392
E-mail: Margus.Kodu@ut.ee

Education

2007–2011	University of Tartu, Faculty of Science and Technology, PhD
2005–2007	University of Tartu, Faculty of Physics and Chemistry, materials technology, MSc, *cum laude*
2001–2005	University of Tartu, Faculty of Physics and Chemistry, materials science, BA
1998–2001	Võru Kreutzwald Gymnasium

Professional employment

2007–...	University of Tartu; engineer
2006–...	Estonian Nanotechnology Competence Centre; researcher
2007–2008	University of Tartu; extraordinary researcher
2005–2007	University of Tartu; lab assistant

Administrative responsibilities

Since 2007	University of Tartu, Faculty of Science and Technology, member of materials science program council

Language skills: Estonian (first language), English (good),
Russian (basic).

ELULOOKIRJELDUS

Üldandmed

Ees- ja perekonnanimi: Margus Kodu
Sünniaeg ja -koht: 16.12.1982, Antsla, Eesti
Kodakondsus: Eesti
Perekonnaseis: vabaabielus, 1 laps
Aadress: Taru Ülikooli Füüsika Instituut,
Riia 142, 51014 Tartu
Telefon: +372 737 4711, +372 5666 7392
e-post: Margus.Kodu@ut.ee

Haridus

2007–2011	Tartu Ülikool, Loodus- ja tehnoloogiateaduskond, materjaliteaduse doktorantuur
2005–2007	Tartu Ülikool, Füüsika-keemiateaduskond, materjalitehnoloogia magistrantuur, kiitusega
2001–2005	Tartu Ülikool, Füüsika-keemiateaduskond, materjaliteaduse bakalaureus
1998–2001	Võru Kreutzwaldi Gümnaasium

Teenistuskäik

2007–...	Tartu Ülikool; insener
2006–...	Eesti Nanotehnoloogiate Arenduskeskuse AS ; projektitäitja
2007–2008	Tartu Ülikool; erakorraline teadur
2005–2007	Tartu Ülikool; laborant

Muu teaduslik organisatsiooniline ja erialane tegevus

Alates 2007	Tartu Ülikooli Loodus- ja tehnoloogiateaduskonna materjaliteaduse õppekava programminõukogu liige.

Keelteoskus: Eesti keel (emakeel), inglise keel (hea), vene keel (algteadmised).

DISSERTATIONES SCIENTIAE MATERIALIS UNIVERSITATIS TARTUENSIS

1. **Martin Järvekülg.** Tubular microstructures by Hf-, Zr- and Ti butoxide gel sheet rolling. Tartu, 2011, 112 p.
2. **Sergei Vlassov.** Investigation of nanoscale interactions and mechanical properties of nanostructures using quartz tuning fork based real-time measurements. Tartu, 2011, 171 p.